Highlights

- optimisation based on a combination of neural networks and evolutionary algorithm
- selected buildings with different midpoint configurations with zero carbon impacts
- regulated energy could be offset with minimal asymmetry
- with operational energy included the structures could be offset with asymmetry
- this method could be expanded to include more building locations and orientation

Topographical optimisation of single-storey non-domestic steel framed buildings using photovoltaic panels for net-zero carbon impact

Ross McKinstray, James B.P. Lim, Tiku T. Tanyimboh, Duoc T. Phan, Wei Sha*, Alexander E.I. Brownlee

* Corresponding author

Ross McKinstray: SPACE, David Keir Building, Queen's University, Belfast, BT9 5AG, UK

Email: rmckinstray01@qub.ac.uk

James B.P. Lim: SPACE, David Keir Building, Queen's University, Belfast, BT9 5AG, UK. Email: j.lim@qub.ac.uk

Tiku T. Tanyimboh: Department of Civil and Environmental Engineering, University of Strathclyde, Glasgow, G1 1XJ, UK. Email: tiku.tanyimboh@strath.ac.uk

Duoc T. Phan: Department of Civil Engineering, Universiti Tunku Abdul Rahman, Kuala Lumpur, 53300, Malaysia. Email: phantd@utar.edu.my

Wei Sha: SPACE, David Keir Building, Queen's University, Belfast, BT9 5AG, UK. Email: w.sha@qub.ac.uk

Alexander E.I. Brownlee: Division of Computing Science and Mathematics, University of Stirling, Stirling, FK9 4LA, UK. Email: sbr@cs.stir.ac.uk

Ross McKinstray, PhD student

James B.P. Lim: PhD, Lecturer

Tiku T. Tanyimboh: PhD, Senior Lecturer

Duoc T. Phan: PhD, Assistant Professor

Wei Sha: PhD, Professor

Alexander E.I. Brownlee: PhD, Senior Research Assistant

Abstract

A methodology is presented that combines a multi-objective evolutionary algorithm and artificial neural networks to optimise single-storey steel commercial buildings for net-zero carbon impact. Both symmetric and asymmetric geometries are considered in conjunction with regulated, unregulated and embodied carbon. Offsetting is achieved through photovoltaic (PV) panels integrated into the roof. Asymmetric geometries can increase the south facing surface area and consequently allow for improved PV energy production. An exemplar carbon and energy breakdown of a retail unit located in Belfast UK with a south facing PV roof is considered. It was found in most cases that regulated energy offsetting can be achieved with symmetric geometries. However, asymmetric geometries were necessary to account for the unregulated and embodied carbon. For buildings where the volume is large due to high eaves, carbon offsetting became increasingly more difficult, and not possible in certain cases. The use of asymmetric geometries was found to allow for lower embodied energy structures with similar carbon performance to symmetrical structures.

Keywords: Portal frames; Genetic algorithms; Artificial neural network; Optimization; Energy efficiency

1 Introduction

Photovoltaic panels (PV) are being used increasingly to reduce the carbon impact of new single-storey industrial buildings. This paper investigates the application of PV panels in conjunction with an asymmetric building shape to optimise the design of a single-storey building for net-zero carbon (Figure 1).

The United Kingdom (UK) has a legal commitment to an 80% reduction of greenhouse gases by 2050 compared to 1990 levels [1]. Of these emissions, approximately 45% of the carbon dioxide (CO_2) is attributed to buildings [2] while 18% of the UK's total emissions are attributed to non-domestic buildings [3]. In order to meet the 2050 target the UK government has projected that the building sector as a whole would need to be almost net-zero carbon [4].

Through new and tighter building regulations it is expected that all new residential buildings will be net-zero carbon from 2016 under level six of the Code for Sustainable Homes and from 2019 for commercial buildings [5, 6]. This will account for an estimated 30% (maximum) of buildings by 2050 dependent on the replacement rate [7]. Any new building should have the lowest environmental impact whilst still performing well as a building. The industry has expressed concerns as to whether these targets are achievable; it has been observed that there are significant gaps between the aspirations and realities foreseen by the sector [8].

One of the most common structural types of non-domestic building is steel portal frames that account for 90% of single-storey commercial buildings in the UK [9]. In the UK, these buildings are normally rented and used for a variety of occupancy types and end uses. In order for a building to be net-zero carbon, the building must offset or mitigate its carbon emissions. In principle, this can be done in two main ways, i.e. either through on-site renewables or by offsetting the building's carbon by investment in an external carbon saving scheme (for example offshore wind). In reality it will depend very much on the legislative definition of net-zero carbon at the planning stage, which is still uncertain.

Three different levels of net-zero carbon offsetting compliance are considered in this paper as follows.

- Regulated carbon offsetting
- Regulated and unregulated carbon offsetting
- Regulated, unregulated and embodied carbon offsetting

Regulated energy is the energy used in the heating, cooling and lighting of a building. Unregulated energy is used in industrial processes, electrical appliances and equipment [2]. The embodied energy and carbon is a tally of the materials used in the construction of the building. Regulated energy is the current standard in determining whether a building has achieved net-zero carbon status through offsetting by renewable energy sources. The wide variety of building end-uses and consequent uncertainty at the design stage makes it difficult to determine unregulated energy. For rented buildings in particular, uncertainty about end-use at the design stage is common. Where a building changes ownership, the unregulated energy usage might change dramatically.

Non-domestic buildings in industrial or commercial areas have a limited number of renewable energy generation options available. A consortium of UK organisations found that out of all building types, single-storey buildings have the greatest potential to achieve net-zero carbon [10]. This can be attributed in part to the topography of the building as the ratio of the roof surface area to usable floor area is relatively very large.

This paper investigates how the optimisation of the building topography in conjunction with PV panels on the roof can be used to achieve net-zero carbon. The building topography can be adjusted to maximise PV panels on the southward side by varying the midpoint ratio (Figure 1). Photovoltaic panels are confined to the building rather than placing additional panels on adjacent land or on the front facade. Where a building is unable to achieve net-zero carbon through roof based PV, additional capacity could be placed on the south facing wall or external on-site structures. However these additional options are not considered in this article. Some other common properties of low-carbon buildings include high efficiency/air tight materials; the use of sky lights in conjunction with tri-dimming control; high efficiency lighting; and the use of passive cooling.

Photovoltaic technologies can be integrated into existing building designs normally as part of the roof with no additional sound pollution. The alternatives, such as wind and geothermal, have significant disadvantages in comparison. For example, wind turbines

require satisfactory wind speeds along with residential buffers to reduce the sound pollution impact on local residents. This tends to preclude their adoption in a significant proportion of the UK, particularly inland and in proximity to urban areas.

In this paper, a large retail unit is considered, since it is the most likely scenario where both unregulated and embodied energy could be accounted for due to the relatively low operational energy and the high number of occupiers willing to accept additional cost for lower carbon impact. Annual energy renewable energy production yields and building energy usage, including building comfort values, are calculated using the dynamic energy simulation package EnergyPlus [11].

As part of a decision support system, simulation-based optimisation has potential to assist the designer. This paper proposes a novel methodology to optimise the design of high efficiency asymmetric single-storey buildings for net-zero carbon incorporating many of the low carbon technologies outlined in previous studies of symmetric structures [10]. This paper focuses on a steel framed building. However the methodology proposed is generic and the frame could be made of other materials.

2 Literature review and optimisation framework

2.1 Literature review

Surveying the literature, examples of domestic building carbon optimisation exist [12, 13], including the more advanced information driven optimisation [14]. However few examples exist of topography optimisation coupled with dynamic energy modelling. Furthermore, there is little work on surrogating multiple objectives as in the approach proposed here with artificial neural networks.

Building energy optimisation has been well-established, with genetic algorithms (GAs) being the dominant form [15, 16]. GAs are very effective in building optimisation due to their capability of handling both continuous and discrete variables. GAs are also very robust in handling discontinuity, multi-modal and highly constrained problems without being trapped at a local minimum [17]. As GAs operate on populations of candidate solutions, a high degree of parallelisation can be leveraged for very efficient implementation including multiobjective optimisation based on Pareto dominance.

For example, low energy homes have been optimised for annual energy consumption in Sydney [18]. This example included multiple building geometries and material parameters as design variables. Also, dwellings have been optimised over their lifecycle [19] considering the embodied energy and cost benefits. The shape of the building has also been considered taking account of building volumes and geometries [20]. In these cases Multi Objective Evolutionary Algorithms (MOEAs) have been used with Pareto-dominance to handle the optimisation of multiple objectives simultaneously.

A genetic algorithm requires thousands of energy simulation runs (i.e. function evaluations) to reach an optimum solution. This is a very computationally intensive and time consuming endeavour. Indeed it is common practice to execute an evolutionary optimisation algorithm multiple times to increase the likelihood of identifying near optimal solutions.

An established method of mitigating the excessive time requirements of the optimisation is to use a response surface approximation model (RSA) in conjunction with a GA [21-24]. This significantly reduces the computational time required for each function evaluation by running the optimisation from the RSA model rather than directly from an EnergyPlus simulation. Thus fast optimisation of different factors multiple times within realistic time constraints can be achieved whilst maintaining a reasonable accuracy with respect to the actual EnergyPlus simulations. There are multiple different types of RSA. A feed forward artificial neural network (ANN) [25] was chosen as it has been previously shown to be accurate in building optimisation studies [21-24].

2.2 Optimisation framework

The optimisation framework of this study is summarised in Figure 2. It is divided into two sequential steps. EnergyPlus is used to generate a large data set for a variety of parameters and configurations outlined in Table 1. This data set is then used to train and validate the ANNs. The ANN is trained on a wide range of building configurations. However, individual optimisations use fixed column heights and spans, with the glazing areas and insulation thicknesses varied by the optimisation engine. Subsequently, as an extension to the optimisation problem solved, in Subsection 5.2, the midpoint ratio is allowed to vary as an additional design variable the value of which is also optimised.

It was found that a single network encompassing all of the identified inputs and target outputs performed very poorly for various reasons e.g. a disjointed relationship between specific inputs and outputs. Therefore, parameters that could be represented easily using a linear relationship from single input variables were removed and replaced with linear equations. For the remaining variables, individual tailored ANNs were used.

3 Description and simulation of the building

A single-storey portal frame building located in Belfast (UK) is considered in this article. The length of the building is 200m with spans of 20m to 50m and column heights of 4m to 10m. The building is south facing with skylights on both sides. The southward side is the store front with a glass façade (see the EnergyPlus model in Figure 3. The building has a large PV system on the south side, covering the maximum possible southward roof area available. The heating, ventilation and cooling (HVAC) system comprises of a gas air handling unit. The building has no direct cooling, relying upon natural ventilation for passive cooling in the summer.

A computer model of a single-storey building was developed in EnergyPlus. The simulation was carried out over an annual period with a 6-25 (min/max) number of start-up days and a time step of 15 minutes. Annual weather files for the Belfast location were used [26].

3.1 Design variables

3.1.1 Building usage

It is assumed that the building is a large retail store or split into multiple stores with identical usage and opening hours (see Table 2). The building has an occupancy of 0.1169 persons/m^2 during periods of occupancy. The building is conditioned by a natural gas air-handling unit with a coefficient of performance (COP) of 0.65 [27], operating from 7am (i.e. two hours before occupancy) to a set point of 23^{o}C.

It is assumed that the building is not actively cooled. In addition to a minimum fresh air per person of 34m^3/h, where temperatures exceed the natural ventilation set point of 24^{o}C, an air exchange rate of up to 6 ACH is utilised. It is assumed that automated louvers in the roof and walls are installed in sufficient quantities to achieve this air exchange rate.

No provision is made for mechanically driven natural ventilation. During periods of high ACH, the building would still be occupied. There are a number of solutions available for achieving the high ACH rate including e-stacks [28] and automated louvers. The impact of high ACH rates on the occupants can be minimised [29]. However, this was not directly considered in the present study. Hot water is provided by an instantaneous hot water only supply with COP of 0.85 and a delivery temperature of 65^{o}C. Water usage is calculated based on an assumed usage of 0.0102l/h/m^2 during occupied hours. The building is lit electrically using suspended tri-step high efficiency LED lighting with a lighting energy of 4W/m^2. The lighting stepping is controlled by a single sensor placed in the centre of the building and offset so as not to be directly under a skylight.

3.1.2 Building construction

The building envelope consists of a steel skinned polyisocyanurate (PIR) core cladding system, where the thickness of the core is variable and coupled with best practice double glazing. The infiltration rate is determined based on proprietary testing values for PIR based cladding products. This is modified to include an approximation of the infiltration of doors and windows. In this study, a value of 1.1m^3/m^2/h is used. Infiltration for cladded buildings has been calculated previously at 0.32m^3/h/m^2 [30]. However, this does not include the high number of openings required for natural ventilation through automated opening windows and louvers. Based on the above surface infiltration rate, the total building ACH is calculated from the internal volume and total building surface area (total side walls, gable walls and roof).

The glazing in the skylights in the roof and the south wall is double glazing with low solar gain with high light emission. It is constructed from based on best practice consisting of two layers of 6mm glass (external colour, internal clear) with a 13mm air gap. The size of the roof glazing for the north and south sides of the building is considered separately, specified as a ratio of roof surface area. Within the model this area is represented with seven thin longitudinal windows, representing multiple windows that would run parallel to the span (see Figure 3).

A photovoltaic system is implemented with a peak operating capacity of 200W/m^2. This is fed into a simple power inverter with an efficiency of 15%. It is assumed that no energy is stored on site but bought and sold on the grid as required. This is represented by 8 large

panels placed on the southward side of the building. The maximum available PV is utilised, based on the area used for glazing and an additional 10% for window frames a PV support structures. Annual photovoltaic energy generation yields are calculated through EnergyPlus, with the predicted value used in the carbon offsetting.

3.2 Embodied energy and carbon

3.2.1 Building energy conversion

Table 3 shows the unit conversion factors for carbon ($kgCO_{2e}$) and energy consumed by the building [31]. EnergyPlus predictions of energy are annual totals. For comparative purposes, energy is converted into thousand watt hours per meter squared floor area over 1 year's operation (kWh_{PA}/m^2) and kilograms carbon dioxide equivalent per meter squared floor area over 1 year's operation ($kgCO_{2e}/m^2$). The conversion factors for grid electricity were used to determine carbon generated by the PV system used in carbon offsetting.

3.2.2 Embodied energy and carbon calculation

Table 4 shows the embodied energy (EE) and carbon (EC) values calculated for the building. These values are based on a range of sources [32-35] that are considered sufficiently accurate for the comparisons made here. Values based on cradle to gate methods were used due to the difficulty in determining disposal and waste streams and the general availability of cradle to gate values. Additionally, the construction, maintenance, fixture and fitting phases of the building life cycle are omitted.

The cladding values are interpolated based on existing Environment Product Declarations (EPD) [32]. These are modified to include the variation in the thickness of the polyisocyanurate (PIR) foam. PIR is chemically similar to polyurethane, allowing for the substitution of values taken from the ICE database [33]. The windows and skylights are taken directly from a glazing facade system EPD [34]. Photovoltaic values are for a CdTe PV system, which have a very short energy payback time and some of the lowest environmental impacts compared to other types of solar technologies [35].

Steel weight values for fabricated sections include an average recycled content [33]. No account is taken for the additional fabrication and welding of the steel into frames. Primary steel member weights are based on optimum primary frame weights for symmetric portal frames using rolled sections [36]. Where the building is asymmetric, a linear presumptive

penalty is used for primary member weight. The penalty is calculated based on a linear assumption that a 0.75 midpoint will have 20% more weight. It is assumed that the purlins and side rails that support the cladding have a constant mass of 4.5kg per m^2 of the building envelope (roof, gables and sides). From this assumption the embodied energy is calculated based on the Coil (Sheet), Galvanised - UK (EU) Average Recycled Content [33].

The building is assumed to have a 125mm concrete floor slab, including the screed insulated with 240mm of insulation. It is assumed that 0.5% of the slab is reinforced with steel rebar. The floor slab is calculated based on the volume of materials using the Bath ICE database values [33]. Pad volumes are calculated based on the assumption that the pad foundation system is governed by uplift caused by the wind. The volume of the concrete pad foundation is calculated based on a column spacing of 6m and an uplift force of 0.5kN/m^2 (1kN/m^2 uplift and 0.5kN/m^2 self-weight). Each pad is assumed to be reinforced with 1% steel reinforcement.

3.3 Selection of the ANN variables and training data

A range of building geometries is considered. The number of decision variables is kept to a minimum in order to reduce the size, complexity and number of EnergyPlus simulations required. This is achieved by omitting HVAC design variables and control parameters, such as heating set points that fall outside the scope of this study. A grid sampling plan (Table 1) totalling 224,000 unique EnergyPlus models was run for 8 different decision variables. The primary topographical variables are the span, column height and midpoint. The building fabric construction variables include the percentage glazing on the roof and front wall. The core thickness of both the wall and the roof is also included independently. The percentage glazing of the north and south roof parts is varied separately to give better solar and heat loss control.

From each EnergyPlus simulation the energy used for heating, lighting and equipment within the building was determined, as well as the PV generated energy. In addition to the energy usage, the building's thermal comfort was determined in three ways:

i. ASHRAE simple method counting the number of hours discomfort for summer and winter clothing during periods of occupancy
ii. The number of occupied hours in excess of 28^{o}C

iii. Fanger Model based on number of occupied hours where the PMV exceed 0.5

The primary comfort concern is overheating as the majority of building occupants in retail environments may be wearing outdoor clothing. Low building temperature discomfort was less of a concern due to the high activity level of the occupants and the availability of additional layers of clothing. Additionally, due to the simplified HVAC implementation, the model would always meet the heating set point temperature. The optimisation does not extend to variables that could influence the number of cold discomfort hours, for example, heating set points or ventilation rates.

4 Artificial neural network and optimisation models

4.1 ANN training

It was found that a single network incorporating all of the identified inputs and target outputs performed very poorly due to the large variation and sometimes disjointed relationships between the inputs and outputs. So multiple single objective ANNs were used, training performance was further improved by eliminating input variables with no relationship to the output variable as well as selecting a training method best suited to the output parameters characteristics. The networks comprised of six or eight neurons in the input layer (corresponding to input variables). The internal light energy target ANN output required six inputs: span, column height, frame midpoint ratio, front wall window %, and skylight % area for both north and south sides. The three remaining target outputs, District Heating, ASHRAE and Fanger PMV, have the core wall insulation thickness of the wall and roof as additional input variables. The recorded model outputs and surrogacy methods are outlined in Table 5. It was found that a single neural network incorporating all of the identified inputs and target outputs was too complex and performed very poorly. The internal equipment, water system heating and photovoltaic energy were predicted using linear equations. The neural networks for ASHRAE discomfort hours and the predicted mean vote (PMV) were generated individually using Bayesian regularisation [37] with 10 neurons using a random 70% of the data set for training and the remaining 30% for testing. Interior lighting and district heating targets were also individually generated using the Levenberg-Marquardt training method with 10 neurons using 60%, 20%, 20% of the data set for

training, validation and testing, respectively. Training methods were selected experimentally. The noisier data sets were trained with Bayesian regularisation which is more capable of dealing with noise [37].

It was not possible to surrogate the total number of occupied hours in excess of 28^{o}C. In practice, however, this requirement is not essential in the present study, as explained in Section 4.4.2.

4.2 Validation

The regression plots between the simulated targets and ANN outputs for the entire initial data set are given in Figure 4. A good agreement can be seen with a regression coefficient above 0.99 for training and validation points combined.

Two additional validations were made to a Latin hypercube sampling (LHS) group and retrospectively to the Pareto curve optimum points in Figure 5. The LHS group consisted of 4000 validation models generated within the constraints of the initial grid data set. The LHS relative error values are shown in Table 6. The relative error values are 1.7% for the internal lighting, 0.6% for heating and 8.8% for ASHRAE thermal comfort. The PMV prediction is less reliable but still reasonable for design purposes. The larger relative error in predictions of the PMV can be attributed to the high sensitivity of discomfort hour prediction methods, causing sudden variation in simulation values.

Figure 5 had 1848 Pareto points which were simulated in EnergyPlus and compared to the ANN result. The R^2 values are reported in Table 5, with above 0.98 values indicating a very good correlation between EnergyPlus and the ANNs. Therefore, the ANN predictions can be considered good enough for design optimisation.

It is uncertain how the proposed methodology will scale to larger design problems, but this would require an increase in the training data size. The methodology is most applicable to small confined problems (at least until it is further developed) where the size of the required training set can be kept manageable.

4.3 Optimisation model

The carbon impact of the building is calculated by converting the regulated and unregulated energies into equivalent carbon values. This is then offset by subtracting the carbon equivalent of the energy produced by the photovoltaic panels (Equation 1).

Carbon Impact = Regulated + Unregulated + Embodied – Offset (1)

A number of limits for overheating have been proposed including a limit of 80 occupied hours exceeding 28^{o}C [38]. Within this study this limit was never exceeded so the constraint was not considered. This can be attributed to the relatively mild weather in Belfast and that the naturally ventilated air was not in excess of 28^{o}C. If the location was in a sunnier warmer part of the UK or Europe this constraint would become a significant factor in the determination of an appropriate building configuration.

In general, minimising the number of uncomfortable hours within the simulation is recommended. Due to the simplified heating system, the set point temperature of 23^{o}C was always met. Discomfort caused by cold within the ASHRAE can be a significant portion of the discomfort. This occurs particularly in the morning, as the building humidity is balancing due to the addition of conditioned air after the period overnight of no conditioning. It is assumed that during these cold periods, occupants would adjust their clothing levels, reducing the impact of cold discomfort. Therefore a limit of 10% occupied hours for ASHRAE and 5% for PMV exceeding 0.5 is adopted, resulting in 327 and 163 hours respectively for the 3276 hours that the building is occupied annually (Equation 2).

In this paper, the MOEA applied is a variant of NSGA-II [39] as implemented by MatLab [40]. The population size was 500. The relatively large population size allowed for better consistency and the generation of enough Pareto points to distribute across the curve including the extremes. This is beneficial during the parametric study as it ensured intermediate points on the curve can be interpolated accurately. The GA operators were intermediate crossover and adaptive feasible mutation. The intermediate crossover creates offspring by taking a weighted average of the parents and adaptive feasible mutation creates a new individual that satisfies the problem bounds. A full MOEA configuration is summarised in Table 7. More details can be found in [40].

Where buildings fall outside these ranges of thermal comfort, a two-step penalty function is applied (Equation 2). The optimisation considers two objectives that are minimised: O_A and O_B, the carbon impact (Equation 1) and embodied carbon respectively, which are scaled by the penalty p depending on the values of ASHRAE and PMV:

$$O_A = Cw$$

$$O_B = Ew$$

where:

$$p = \begin{cases} 1 & if\ \ ASHRAE < 327\ h\ and\ PMV < 163\ h \\ 10 & if\ \ 327h < ASHRAE < 654\ h\ \ or\ \ 163h < PMV < 326\ h \\ 100 & if\ \ ASHRAE\ > 654\ h\ \ or\ \ PMV > 326\ h \end{cases} \quad (2)$$

5 Results and discussion

5.1 Example building

A frame of span 40m and column height of 5m is considered with 30% frontal glazing. The building is optimised using two objectives: carbon impact and total embodied carbon. There are four decision variables:

- North roof % skylights
- South roof % skylights
- Wall core insulation thickness
- Roof core insulation thickness

For the three carbon impact calculation options, Pareto curves are produced for carbon impact and embodied carbon with midpoint ratio ranging from 0.5 to 0.8 at 0.05 intervals, (see Figure 5). Embodied carbon values are calculated per annum assuming a 30 year building life, as at this point in the building's life major components, including the PV system, will need to be replaced. It is assumed that the replacement materials will be offset by the replacement renewable energy system.

It can be seen for all optimisations that as carbon usage is reduced, the embodied energy exponentially increases. This is characteristic of the diminishing returns of increased insulation on reduction of building heating costs. This is the main finding of the

optimisation. For the Belfast location to achieve regulated net-zero carbon offsetting it is clear that asymmetric building shapes are not required. However, if operational energy is included a midpoint ratio of 0.55 to 0.6 would be beneficial (although not required). In Figure 5 a symmetric 0.5 midpoint configuration could be net-zero carbon but would consume significantly more resources than an equivalent performing frame with a 0.6 midpoint ratio. When embodied carbon is included the necessary degree of asymmetry is increased significantly, with a midpoint ratio of 0.75 or larger required. This shows how the designer can identify net-zero carbon impact buildings solutions where symmetric configurations do not exist through asymmetry and reduce the embodied carbon of those solutions.

For each of the carbon Pareto curves in Figure 5 the equivalent embodied and operational energy curves were produced (Figure 6). There are significant differences between the carbon and energy in achieving net-zero energy offset status. This is due to the difference in carbon to energy conversion factors for the different energy streams. A significant proportion of the building's energy usage is attributed to the gas heating which has significantly lower carbon impact than utilising grid electricity. This resulted in a significantly larger effort being required to offset the regulated energy requiring a 0.75 midpoint. A large number of buildings configurations with small roof surface areas to volume failed to achieve net-zero energy offsetting with any midpoint.

An example carbon calculation is shown for a point selected from Figure 5 for a building offset using the regulated, unregulated and embodied carbon criteria. As embodied carbon is an indicator of material quantities, and therefore a cost, the lowest possible embodied carbon is advantageous. The 0.8 midpoint curve is selected as it has relatively low embodied carbon that is not within the steep exponential gradient.

The building has a span of 40m, column height of 5m, midpoint of 0.8, front window of 30%, skylights south of 6.3%, north of 16.5% and core insulation thicknesses of 76.2mm walls and 101.6mm roof. The surrogacy predictions of the chosen optimum configuration are shown in Table 8. Table 9 shows the calculation of the carbon impact. The regulated (+19.1 $kgCO_{2e}PA/m^2_{floor}$) unregulated (+6.96 $kgCO_{2e}PA/m^2_{floor}$) and embodied (+9.09 $kgCO_{2e}PA/m^2_{floor}$) carbon are offset by the PV (-35.1 $kgCO_{2e}PA/m^2_{floor}$) over an assumed 30

year lifetime. The carbon impact is calculated in Equation 1. This results for the chosen exemplar configuration in a carbon impact of approximately net-zero.

A breakdown of both the carbon and energy is shown in Figure 7. It is clear that the most significant building aspect is the heating of the buildings followed by the embodied energy/carbon. The embodied energy of the 30 year lifecycle is significant, accounting for 26% of the carbon within the building. It is therefore important to include this within the design decision making process.

Each GA optimisation run took around 10 minutes CPU time to complete on a Workstation running on a single thread at 3.2GHz. It took approximately 2 weeks to generate the training data set and approximately 3 hours to train each ANN. The function evaluation time of the ANN is under 0.001 second whereas the time to generate, simulate and extract the result of a single EnergyPlus model is 24 to 28 seconds. If the ANN was not implemented and the optimisation was run directly with EnergyPlus, each GA optimisation run would have taken more than 10 days (based on the number of evaluations performed). The time saving associated with ANN based optimisation approach is significant, particularly if the ANN has already been created. Relatively minor modifications to the present methodology, for example adding additional parameters such as roof orientation, would make the ANN reusable for multiple projects for a specific geographic location.

5.2 Parametric study

A parametric study was conducted to identify the necessary building shape modification for a range of building spans and column heights. Buildings were optimised on a grid of 13 spans and 5 column heights across the ANN input range. The insulation core thickness was limited to 200mm in order to prevent configurations with unrealistically high embodied carbon.

In the example building (Figure 5) the objective was to create Pareto curves of carbon impact and embodied carbon for one frame topography with multiple midpoint ratios. In the parametric study the objective is to identify the midpoint ratio for net-zero carbon of a topographical range of spans and column heights. In order to achieve this GA optimisation objectives were reconfigured from the example frame to carbon impact and midpoint ratio. The midpoint ratio was thus added as a fifth decision variable to the optimisation. Embodied

carbon was removed as an objective. Instead its maximum value was limited by the constraint on the insulation thickness. The MOEA was run 5 times. From the Pareto curves produced, a solution equating to net-zero carbon impact was selected with the most symmetric midpoint ratio from the 5 curves. This midpoint is then reported in the contour plots (Figures 8-10). This indicates the extent of asymmetry required to achieve a net-zero carbon impact for different building topographies while still limiting embodied carbon to feasible levels.

Where the building topography failed to meet net-zero carbon at the maximum (0.8) midpoint ratio or meets it under the minimum midpoint ratio (0.5), the carbon impact value is reported in place of the midpoint ratio. The change between contour plot values switching between reporting midpoint and carbon impact values is represented by a thick black line.

The offsetting of regulated carbon was found to be very achievable with the majority of spans and column heights achieving below net-zero carbon status in symmetric shaped buildings. The exception is tall short span frames (Figure 8). This is indicative of the larger heating requirements of taller buildings coupled with limited roof area for carbon offsetting through PV panels. A similar observation can be made about offsetting regulated and unregulated carbon (Figure 9). The low height buildings with long spans achieve below net-zero carbon without asymmetry, whereas the taller and shorter span buildings require some degree of asymmetry to meet net-zero carbon impact.

When embodied energy is included (Figure 10), only low buildings were able to achieve net-zero carbon impact with a significant midpoint offset. Tall buildings offset to the maximum offset ratio of 0.8 had positive carbon impacts of up to $10kgCO_{2e}/m^2_{floor}$. In the cases where the building failed to achieve a net-zero carbon impact, additional methods could be taken. The operational carbon could be reduced by increasing the insulation thickness optimisation upper limit, or more practically, the offsetting carbon can be increased. This can be achieved by incorporating additional PV panels to the front of the building or to additional structures, for example, car park and walkway covers.

6 Conclusion

This paper used an optimisation methodology based on a combination of artificial neural networks and a multi objective evolutionary algorithm. Its aim was to identify the optimal net-zero carbon configurations for novel asymmetric single-storey steel buildings of differing spans and column heights. First, the ANN was trained and validated using simulation results. The database of cases was created using grid sampling followed by multi-objective optimisation in MatLab. The ANN proved to be able to provide acceptable approximations of the simulation results, with average relative errors below 2% for both the total lighting and district heating energy, and below 15% for the average thermal comfort scores.

The optimisation successfully selected buildings with multiple different midpoint configurations with net-zero carbon impacts for different net-zero definitions. The spread of the solutions reflects the large number of potential configurations. The optimisation process was useful in identifying solutions with minimal embodied energy, which not only reduce carbon in buildings but generally decrease the cost of the building due to the reduction in use of materials. This methodology could prove useful not only in identifying the optimum midpoint asymmetry of new buildings but also in the selection of building materials based on their embodied energy.

It was found that regulated energy could be offset with minimal asymmetry; whereas when operational energy was included the majority of structures could be offset successfully with asymmetry. Where embodied energy was included only low frames could be offset without the inclusion of additional PV panels outside the scope of this analysis. This method would be used in designing new single-storey buildings that strive to achieve a completely net-zero carbon impact. With government incentives, PV is very economically competitive and capable of repaying the additional investment over their lifetime. For clients aiming for completely net-zero carbon impact buildings or who have higher regulated carbon requirements caused by inclusion of active cooling, this methodology could be used to provide design solutions that far surpass current building regulations for regulated carbon in a manner where the additional investment can be recovered through additional generated PV energy.

In future work, this method could be expanded to include more building locations and orientations. This will be a particular challenge in locations where thermal gains may

overwhelm the natural ventilation requiring the inclusion of active cooling. The embodied energy could be expanded to include the lighting, heating and cooling systems. Structural steel mass could be improved through a separate structural steel optimisation rather than relying on assumed mass values based on symmetric building designs.

References

[1] Department of energy and Climate change, *Climate change act impact assessment*, no. March. 2008.

[2] UK Green Building Council, "Zero Carbon Task Group Report The Definition of Zero Carbon.," 2008.

[3] Carbon Trust, "Building the future, today : transforming the economic and carbon performance of the buildings we work in," London, 2010.

[4] HM Goverment, "The Carbon Plan: Delivering our low carbon future," 2011.

[5] Green Building Council Registered, "Building Zero Carbon - the case for action Examining the case for action on Zero Carbon Non Domestic Buildings," London, 2014.

[6] House of Commons, "20 Dec 2010 : Column 135WS Written Ministerial Statements," 2010. [Online]. Available: http://www.publications.parliament.uk/pa/cm201011/cmhansrd/cm101220/wmstext/101220m0001.htm. [Accessed: 06-Aug-2014].

[7] UK Green Building Council, "Report on carbon reductions in new non-domestic buildings," 2007.

[8] R. Vaughan, "Government's 2016 zero-carbon home target 'too unrealistic,'" *The Architects Journal*, 06-Mar-2008.

[9] B. Davison and G. Owens, Eds., *Steel Designers' Manual*, 6th Editio. Blackwell Publishing, 2008.

[10] Target Zero, "Guidance on the design and construction of sustainable, low carbon warehouse buildings," 2010.

[11] N. Fumo, "A review on the basics of building energy estimation," *Renew. Sustain. Energy Rev.*, vol. 31, pp. 53–60, Mar. 2014.

[12] W. Wang, H. Rivard, and R. Zmeureanu, "An object-oriented framework for simulation-based green building design optimization with genetic algorithms," *Adv. Eng. Informatics*, vol. 19, no. 1, pp. 5–23, Jan. 2005.

[13] S. Bucking, A. Athienitis, and R. Zmeureanu, "Multi-objective optimal design of a near net-zero energy solar house," *ASHRAE Trans.*, vol. 120, no. 1, 2014.

[14] S. Bucking, R. Zmeureanu, and A. Athienitis, "An information driven hybrid evolutionary algorithm for optimal design of a Net Zero Energy House," *Sol. Energy*, vol. 96, pp. 128–139, Oct. 2013.

[15] A.-T. Nguyen, S. Reiter, and P. Rigo, “A review on simulation-based optimization methods applied to building performance analysis,” *Appl. Energy*, vol. 113, pp. 1043–1058, Jan. 2014.

[16] R. Evins, “A review of computational optimisation methods applied to sustainable building design,” *Renew. Sustain. Energy Rev.*, vol. 22, pp. 230–245, Jun. 2013.

[17] A. Colorni, M. Dorigo, and V. Maniezzo, “Genetic algorithms and highly constrained problems: The time-table case,” *Proc. First Int. Work. Parallel Probl. Solving from Nat.*, pp. 55–59, 1991.

[18] S. M. Bambrook, A. B. Sproul, and D. Jacob, “Design optimisation for a low energy home in Sydney,” *Energy Build.*, vol. 43, no. 7, pp. 1702–1711, Jul. 2011.

[19] G. Verbeeck and H. Hens, “Life cycle optimization of extremely low energy dwellings,” *J. Build. Phys.*, vol. 31, no. 2, pp. 143–177, Oct. 2007.

[20] W. Wang, H. Rivard, and R. Zmeureanu, “Floor shape optimization for green building design,” *Adv. Eng. Informatics*, vol. 20, no. 4, pp. 363–378, Oct. 2006.

[21] L. Magnier and F. Haghighat, “Multiobjective optimization of building design using TRNSYS simulations, genetic algorithm, and artificial neural network,” *Build. Environ.*, vol. 45, no. 3, pp. 739–746, Mar. 2010.

[22] F. Boithias, M. E. Mankibi, and P. Michel, “Genetic algorithms based optimization of artificial neural network architecture for buildings’ indoor discomfort and energy consumption prediction,” in *Building Simulation*, 2012, pp. 1–12.

[23] A. P. Melo, D. Cóstola, R. Lamberts, and J. L. M. Hensen, “Development of surrogate models using artificial neural network for building shell energy labelling,” *Energy Policy*, pp. 1–10, Feb. 2014.

[24] D. Gossard, B. Lartigue, and F. Thellier, “Multi-objective optimization of a building envelope for thermal performance using genetic algorithms and artificial neural network,” *Energy Build.*, vol. 67, pp. 253–260, Dec. 2013.

[25] M. Jianchang and K. J. Anil, “Artificial neural networks: A tutorial,” *Computer (Long. Beach. Calif).*, vol. 29, no. 3, pp. 31–44, 1996.

[26] ASHRAE, “International Weather for Energy Calculations (IWEC Weather Files) Users Manual and CD-ROM GBR_Belfast .039170_IWEC.epw,” Atlanta, 2001.

[27] “When DesignBuilder output is different from unprocessed EnergyPlus Output,” [Online]. Available: http://www.designbuilder.co.uk/helpv4.0/Content/When_DesignBuilder_output_is_different_from_unprocessed_EnergyPlus_Output.htm. [Accessed: 14-Oct-2014].

[28] Breathing Buildings, “Asda adopts ultra low-energy ventilation at Langley Mill,” 2010. [Online]. Available: http://www.breathingbuildings.com/news/latest-news/asda-adopts-ultra-low-energy-ventilation-at-langley-mill. [Accessed: 14-Oct-2014].

[29] Francis Allard (ed.), “Natural Ventilation in Buildings: A Design Handbook.” James & James, London, 1998.

[30] K. Gowri, D. Winiarski, and R. Jarnagin, “Infiltration modeling guidelines for commercial building energy analysis,” U.S. Department of Energy, 2009.

[31] Carbon Trust, “Conversion Factors - Energy and carbon conversions,” London, 2011.

[32] Kingspan, “Product data sheet product: KS1000RW trapezoidal EcoSafe insulated roof panel,” 2013.

[33] C. I. Jones and G. P. Hammond, “Embodied energy and carbon in construction materials,” *Proc. ICE - Energy*, vol. 161, no. 2, pp. 87–98, Jan. 2008.

[34] Schuco, “Environmental Product Declaration Musterobjekt EPD FW,” 2009.

[35] J. Peng, L. Lu, and H. Yang, “Review on life cycle assessment of energy payback and greenhouse gas emission of solar photovoltaic systems,” *Renew. Sustain. Energy Rev.*, vol. 19, pp. 255–274, Mar. 2013.

[36] R. Mckinstray, J. B. P. Lim, T. T. Tanyimboh, D. T. Phan, and W. Sha, “Optimal design of long-span steel portal frames using fabricated beams,” *J. Constr. Steel Res.*, vol. 104, pp. 104–114, 2015.

[37] M. H. Beale, M. T. Hagan, and H. B. Demuth, “Neural Network Toolbox™ Reference R2014a.” MathWorks, Natick, 2014.

[38] Department for Education and Skills, “Guidelines for environmental design in schools,” 2003.

[39] K. Deb, A. Pratap, S. Agarwal, and T. Meyarivan, “A fast and elitist multiobjective genetic algorithm: NSGA-II,” *IEEE T. Evol. Comput.*, vol. 6, no. 2, pp. 182–197, 2002.

[40] MathWorks, “Optimization Toolbox™ User’s Guide.” MathWorks, Natick, 2013.

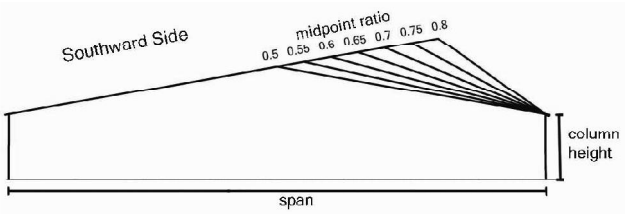

Figure 1 Topographic effect of the midpoint ratio

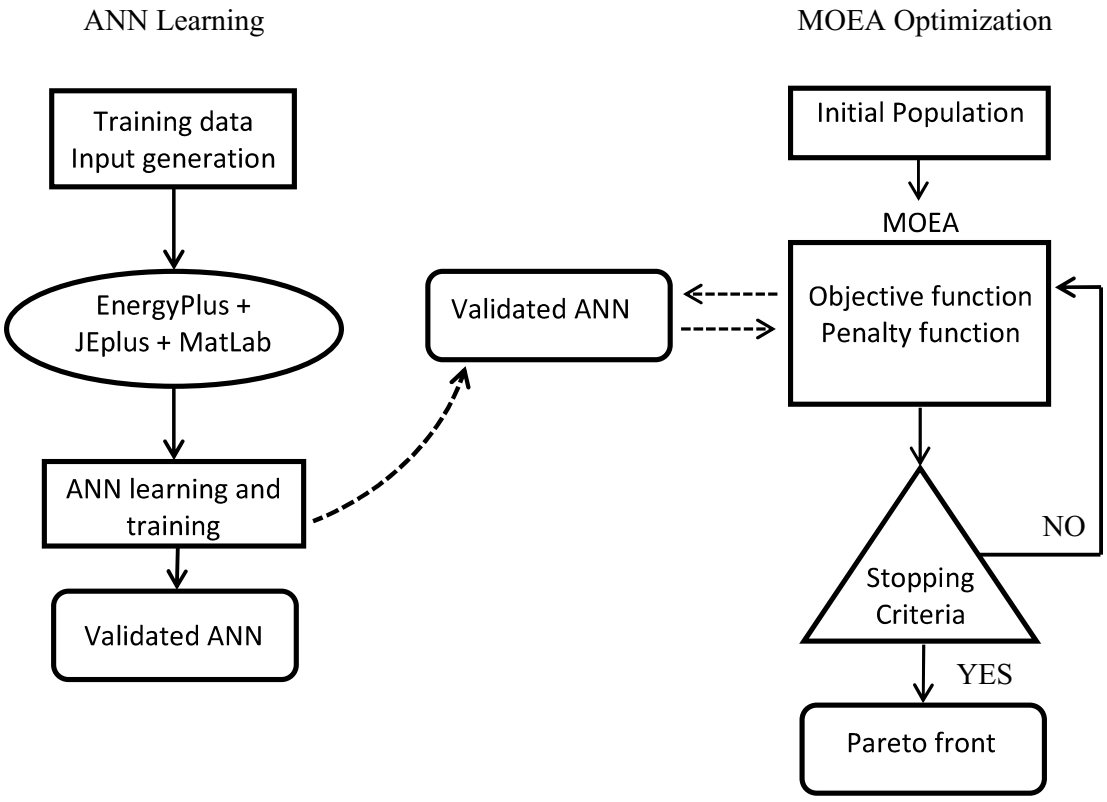

Figure 2 Optimisation framework

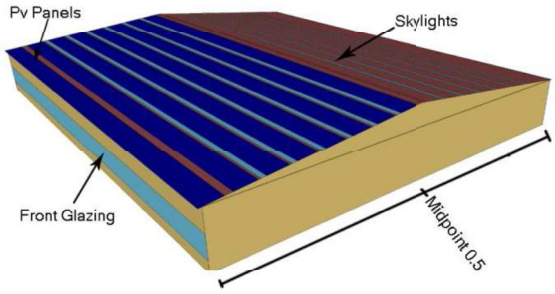

Figure 3 EnergyPlus simulation model representation

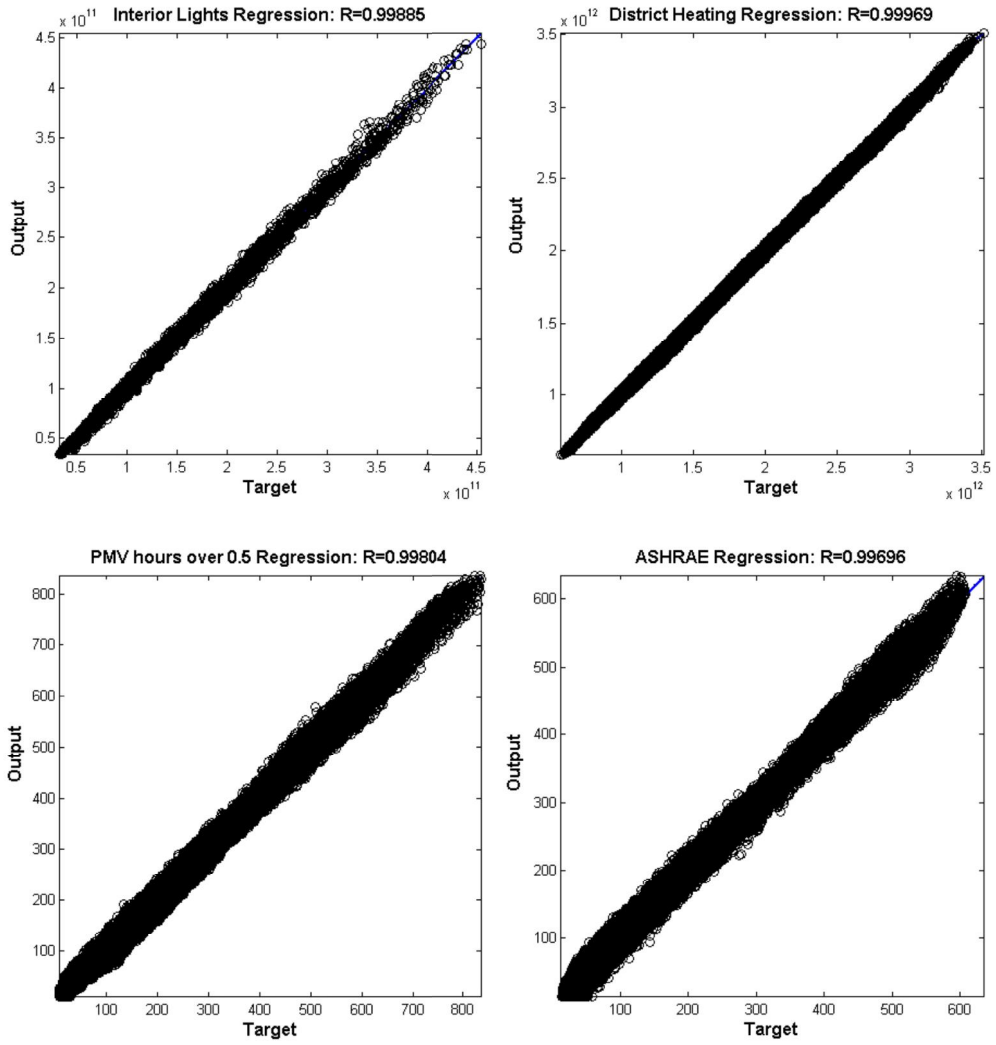

Figure 4 Comparison between ANN outputs and simulated targets

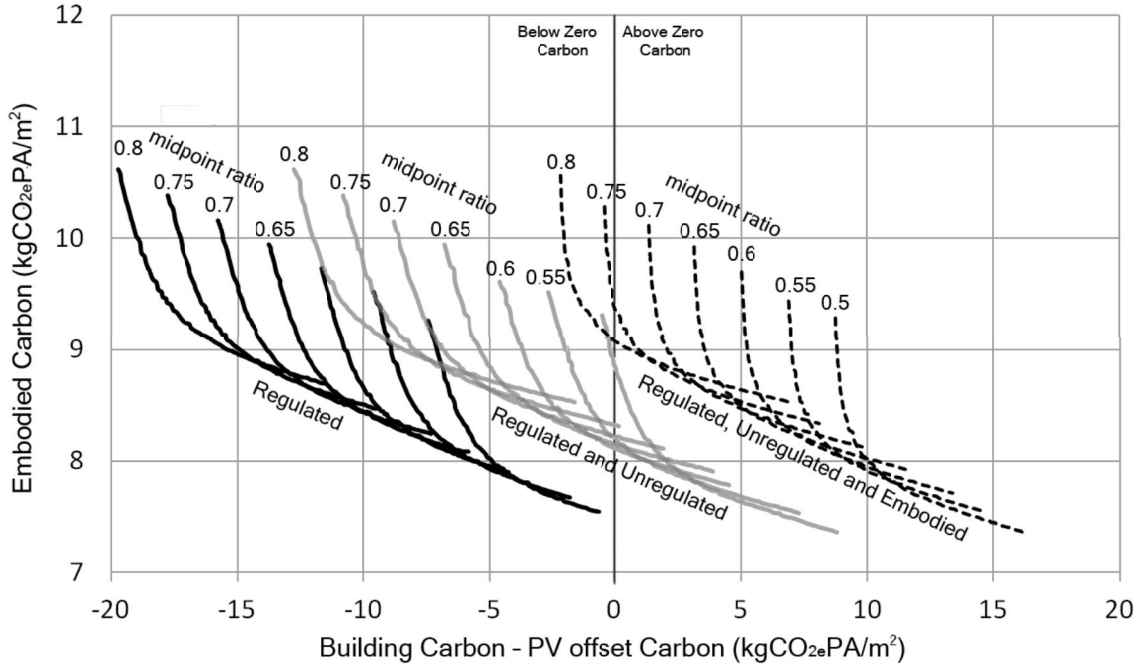

Figure 5 Pareto-optimal curves for different midpoint and carbon objectives

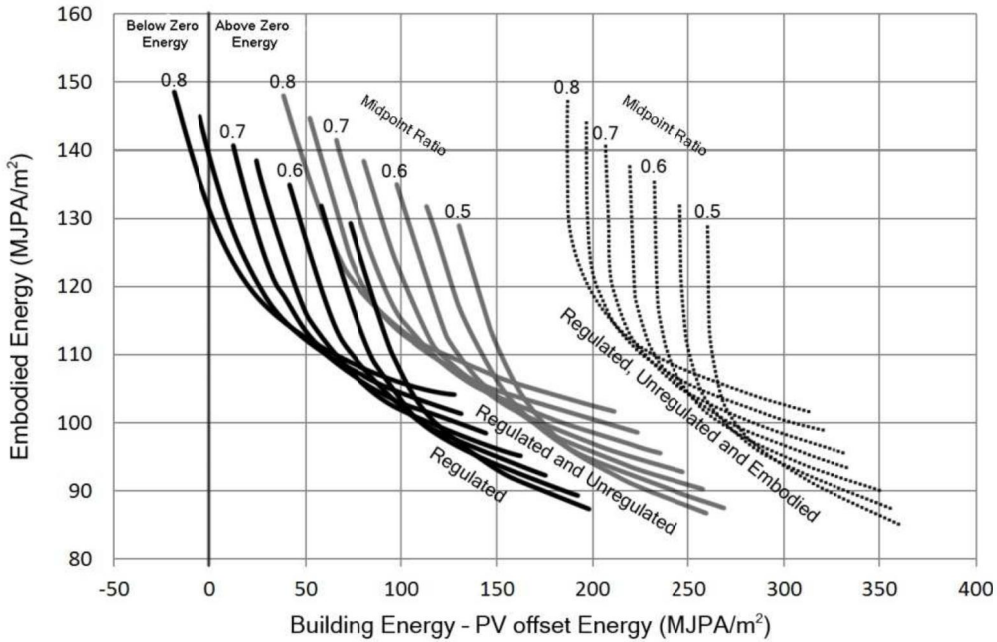

Figure 6 Energy equivalent of the carbon Pareto-optimal curves in Figure 5

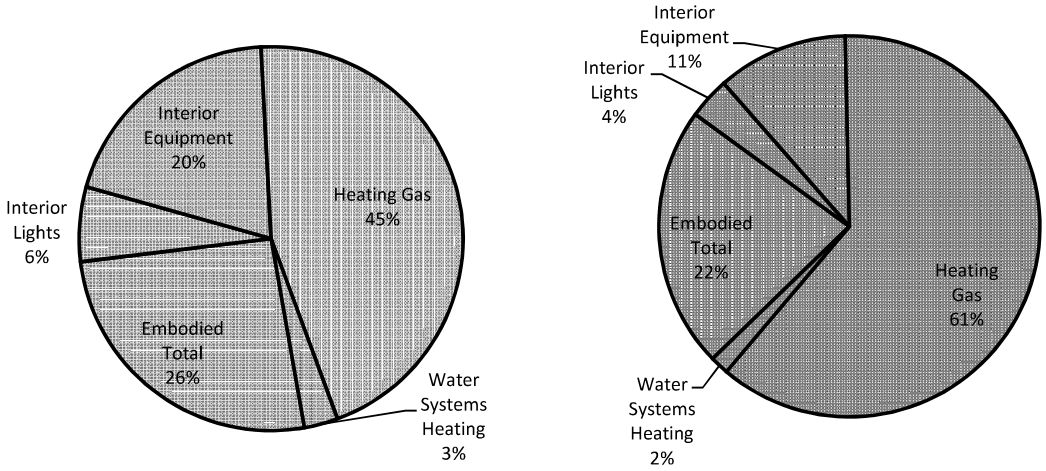

a) Embodied Carbon **b) Embodied Energy**

Figure 7 30 year life time breakdown of building energy and carbon

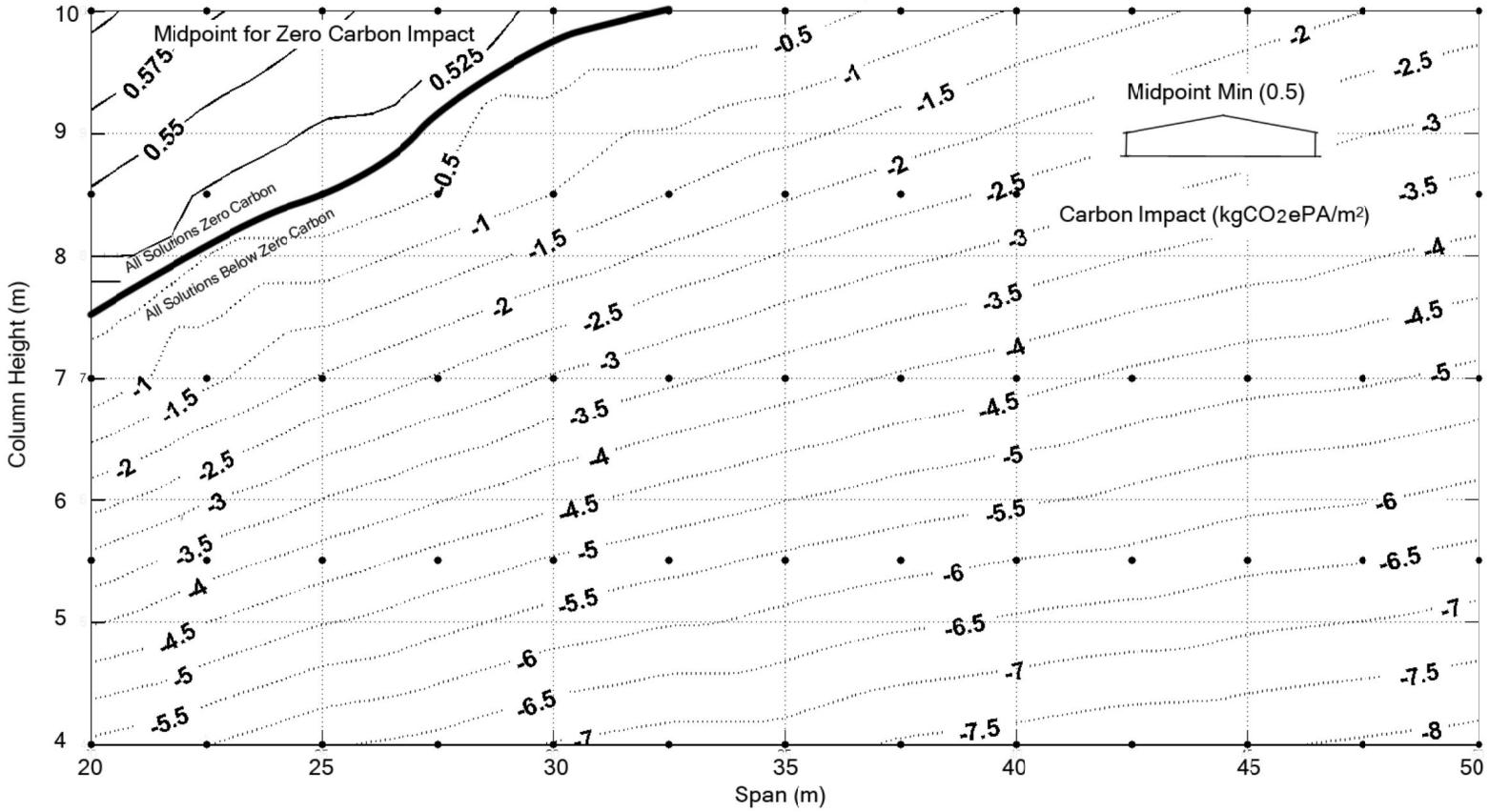

Figure 8 Regulated carbon offsetting

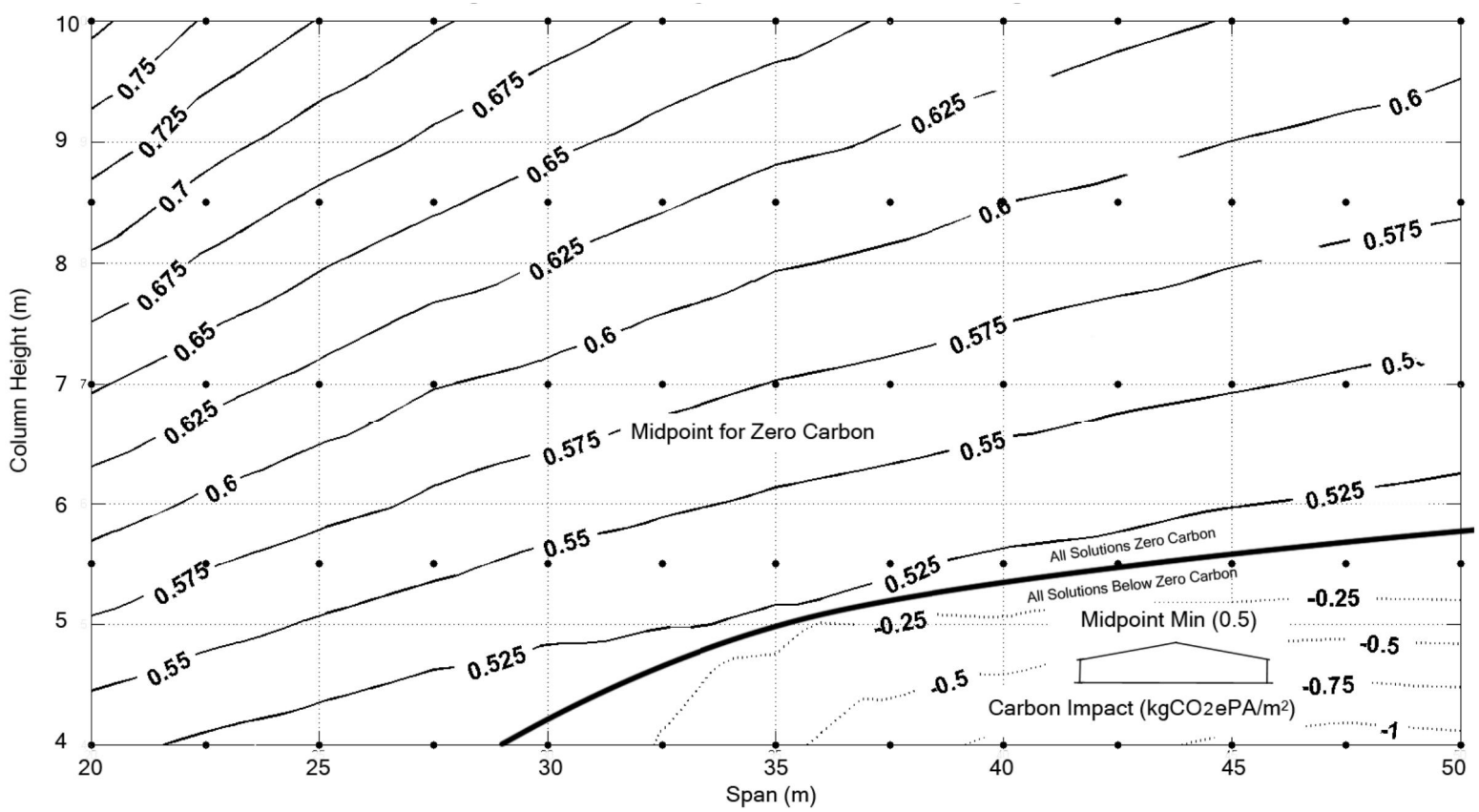

Figure 9 Regulated and unregulated carbon offsetting

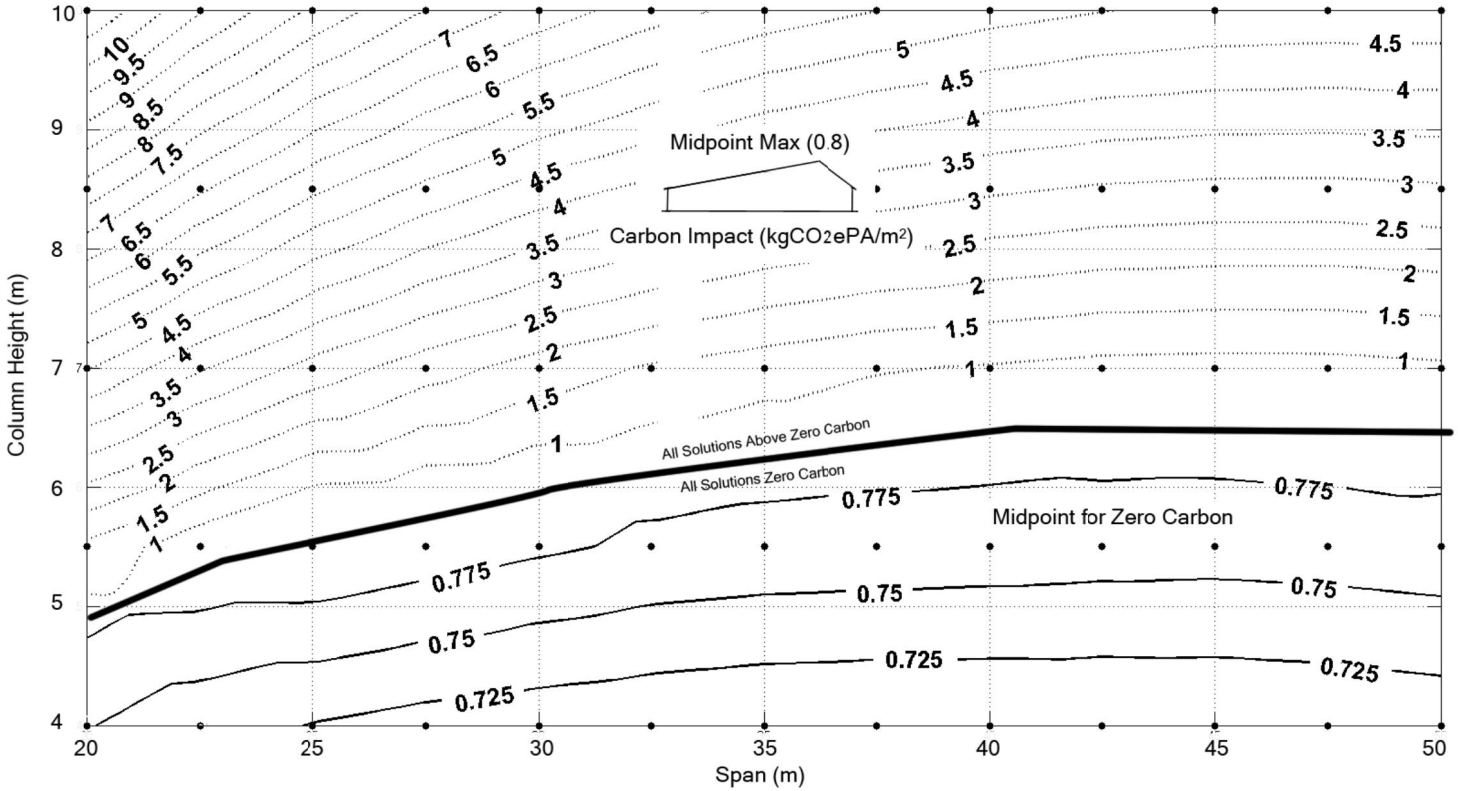

Figure 10 Regulated, unregulated and embodied carbon offsetting

Table 1 Creation of the training data set

Decision variables	Candidate values	Number of options
Span (m)	20, 25, 30, 35, 40, 45, 50	7
Column height (m)	4, 6, 8, 10	4
Model midpoint (ratio)	0.5, 0.575, 0.65, 0.725, 0.8	5
Wall facade glazing (%)	20, 35, 50, 65, 80	5
Skylight south side (%)	2.5, 7.5, 12.5, 17.5, 22.5	5
Skylight side (%)	5, 12.5, 20, 27.5	4
Core thickness wall (m)	0.05, 0.1, 0.2, 0.3	4
Core Roof (m)	0.05, 0.1, 0.2, 0.3	4

Table 2 Occupancy and usage schedule

Time period	Weekdays	Saturdays	Sundays
24:00 Until 09:00	0	0	0
09:00 Until 10:00	0.75	0.75	0.75
10:00 Until 12:00	1	1	1
12:00 Until 14:00	0.75	0.75	0.75
13:00 Until 17:00	1	1	1
17:00 Until 18:00	0.75	0.75	0.75
18:00 Until 24:00	0	0	0

Table 3 Energy conversion factors [31]

Original unit	Embodied carbon ($kgCO_{2e}$)	Embodied energy (MJ)
1kWh	N/A	3.6
UK grid electricity (1kWh)	0.44548 [31]	3.6
Natural gas (1kWh)	0.18404 [31]	3.6

Table 4 Embodied carbon (EC) and Embodied Energy (EE)

Component	EC	EE
Cladding	0.1704xCoreThickness(mm)+49.77 $kgCO_{2e}/m^2_{Envelope}$	4.06xCoreThickness(mm)+305 $MJ/m^2_{Envelope}$
Window/skylights	62 $kgCO_{2e}/m^2_{Window}$	907 MJ/m^2_{Window}
PV	24 $gCO_{2e}/kWh_{generated}$	1300 $MJ/m^2_{PV\ area}$
Primary steel member	1.66 $kgCO_{2e}/kg_{Primary\ Steel\ Member}$	21.5 $MJ/kg_{Primary\ steel\ member}$
Purling's	6.93 $kgCO_{2e}/m^2_{Envelope}$	101.7 $MJ/m^2_{Envelope}$
Floor slab	45.068 $KgCO_{2e}/m^2_{floor}$	474.45 MJ/m^2_{floor}
Foundation	364.1 $kgCO_{2e}/m^3_{foundation\ pad}$	3147.9 $MJ/m^3_{foundation\ pad}$

Table 5 EnergyPlus recorded outputs and surrogacy method

Model outputs	Output surrogacy method	R^2 for the Pareto optimal points in Figure 5
Interior lights electricity [J] (RunPeriod)	Levenberg-Marquardt feed forward ANN with 1 hidden layer with 10 neurons	0.987
Interior equipment electricity [J] (RunPeriod)	5.624×10^7 J/m^2_{floor}	
Heating district heating [J] (RunPeriod)	Levenberg-Marquardt feed forward ANN with 1 hidden layer with 10 neurons	0.999
Water systems district heating [J] (RunPeriod)	6.848×10^6 J/m^2_{floor}	
Photovoltaic electricity produced [J] (RunPeriod)	4.137×10^8 J/$m^2_{PV\ Roof\ Area}$	
ASHRAE 55 simple model Summer or winter clothes not comfortable Time	Bayesian regularization feed forward ANN with 1 hidden layer with 10 neurons	0.988
Air hours over 28 (h)	Not applicable	
Fanger PMV hours over 0.5 (h)	Bayesian regularization feed forward ANN with 1 hidden layer with 10 neurons	0.986

Table 6 Statistical repatriation of relative error in ANN validation

Relative error		<1%	<2.5%	<5%	<10%	<25%	<50%	Average (%)
Percentage of cases when error falls into the range Initial grid/(LHS Sampling Plan)	Interior Lights	40.9/(46.8)	78/(84)	96/(93.6)	99.7/(98.8)	100/(100)	100/(100)	1.699/(1.643)
	District Heating	81.6/(85.3)	98.9/(92.8)	100/(95.3)	100/(98.7)	100/(100)	100/(100)	0.612/(0.916)
	ASHRAE 55 Simple	12.8/(85.3)	30.1/(92.8)	50.3/(95.3)	70.4/(98.7)	92/(100)	99.2/(100)	8.811/(7.977)
	PMV hours over 0.5	27.7/(12.1)	41.8/(28.9)	59.6/(48.7)	74.8/(66.6)	88.2/(80.8)	96/(86.5)	N/A

Table 7 MOEA Configuration

Population size	Selection method	Crossover type	Crossover probability	Mutation type	Termination criteria
500	Tournament	Intermediate	0.8	Adaptive feasible	Maximum number of generations = 300 Stall generations limit = 35

Table 8 Example optimum configuration building energy predictions per annum (from 5 optimisation runs)

	Surrogacy prediction (GJ)	MJ/m^2_{floor}	kWh/m^2_{floor}	$kgCO_{2e}/m^2_{floor}$
Interior lights	142.6	17.83	4.95	2.2
Interior equipment	449.9	56.24	15.62	6.96
Heating gas	2488.1	311.01	86.39	15.9
Water heating	64.5	8.06	2.24	1.0
Photovoltaic electricity produced	2271.3	283.92	78.87	35.1

Table 9 Embodied energy & carbon calculation over 30 year lifetime

Component	Quantity	EC $kgCO_{2e}/m^2_{floor}$	EE MJ/m^2_{floor}
Roof area cladding	7830.59 (m^2)	65.66	702.27
Roof area glass	746.07 (m^2)	5.78	84.59
Roof area PV	5490.71 (m^2)	56.78	892.24
Wall area cladding	2325.70 (m^2)	18.25	178.65
Wall area glass	300.00 (m^2)	2.33	34.01
Envelope area purlin's	11202.36 (m^2)	9.70	142.41
Ground floor slab	8000.00 (m^2)	45.07	474.45
Foundation	0.0212 (m^3/m^2_{floor})	7.72	66.74
Primary steel members	36.98 (kg_{steel}/m^2_{floor})	61.39	795.15
	Totals	272.68	3370.5